

# MULTI-SENSOR/MULTI-TEMPORAL ANALYSIS OF ENVISAT DATA FOR SNOW MONITORING

Rune Solberg<sup>(1)</sup>, Jostein Amlien<sup>(1)</sup>, Hans Koren<sup>(1)</sup>, Line Eikvil<sup>(1)</sup>, Eirik Malnes<sup>(2)</sup> and Rune Storvold<sup>(2)</sup>

<sup>(1)</sup> Norwegian Computing Center (NR) Oslo, Norway, Email: [rune.solberg@nr.no](mailto:rune.solberg@nr.no)

<sup>(2)</sup> NORUT IT, Tromsø, Norway, Email: [eirik.malnes@itek.norut.no](mailto:eirik.malnes@itek.norut.no)

## ABSTRACT

The ENVISAT satellite with its many sensors opens for new, interesting approaches of combined multi-sensor, multi-temporal monitoring. In this study, we have focused on monitoring of snow parameters in the snowmelt seasons of 2003 and 2004 (April-June) in South Norway. The sensors used in this study are ENVISAT MERIS and ASAR and Terra MODIS. The study is motivated by operational prospects for snow hydrology, meteorology and climate monitoring.

We have developed a generic multi-sensor/multi-temporal approach for monitoring of snow cover area (SCA), snow surface wetness (SSW) and snowmelt onset time (SOT). The objective is to analyse, on a daily basis, a time series of optical and SAR data together producing sensor-independent products. We have defined raster products for each variable and developed a prototype production line. The production line automatically performs data retrieval, pre-processing, parameter retrieval, data aggregation and product generation.

A few algorithms for multi-sensor/time-series processing have been developed and are compared. One approach is to analyse each image individually and combine them into a day product. How each image contributes to the day products is controlled by a pixel-by-pixel confidence value that is computed for each image analysed. The confidence algorithm is able to take into account, e.g., information about observation geometry, probability of clouds, prior information about snow state and reliability of the classification. The time series of day products are then combined into a multi-sensor/multi-temporal product. The combination of products is done on a pixel-by-pixel basis and controlled by each individual pixel's confidence and a decay function of time for the product. The "multi-product" should then represent the most likely status of the monitored variable.

## 1 INTRODUCTION

The seasonal snow cover is practically limited to the northern hemisphere. Here, the average snow extent during the winter months ranges from 30 to 40 million km<sup>2</sup>. The water equivalent volume of these snow masses ranges from 2000 to 3000 km<sup>3</sup>. In Fennoscandia and the Alps, snowfall is a substantial part of the overall

precipitation. In Finland 27% of the annual average and in Norway about 50% of the precipitation in mountainous areas is snow.

Snow cover has a substantial impact on the interaction processes between the atmosphere and the surface. Thus, the knowledge of snow parameters is important for both climatology and weather forecast. The snow cover has also an important impact on water hydrology in regions with seasonal snow.

Optical remote sensing sensors are able to map snow cover quite accurately, but are limited by clouds. SAR sensors penetrate the clouds, but current satellite-borne sensors are only able to map wet snow accurately.

The research institutes NR and NORUT IT are currently developing algorithms for snow parameter mapping applying a multi-sensor and multi-temporal approach. The overall idea is to combine the use of optical and SAR sensors and utilise the best features of each sensor when possible in order to map snow parameters more frequently and with better spatial coverage than would otherwise be possible.

In this paper we describe our first experiments with multi-sensor and multi-temporal retrieval of snow cover area (SCA), snow surface wetness (SSW) and snowmelt onset time (SOT). The results reported here include the use of ENVISAT MERIS and ASAR and Terra MODIS. Common for all the experiments is that the sensor fusion has taken place at the level of geophysical parameters. A future topic might be to experiment with fusion at the sensor data level.

## 2 SNOW COVER AREA ALGORITHMS

### 2.1 Parameter retrieval algorithms

The optical SCA algorithm is based on an empirical reflectance-to-snow-cover model originally proposed for NOAA AVHRR in [1] and later refined in [2]. The algorithm has recently been tailored to MODIS data by NR. It retrieves the snow-cover fraction for each pixel. The model is calibrated by providing two points of a linear function relating observed reflectance (or radiance) to fractional snow-cover area. The calibration is usually done automatically by means of calibration areas. Statistics from the calibration areas is then used to compute calibration points for the linear relationship.

Various approaches have been tested for cloud detection, and the best results so far have been obtained using a k Nearest Neighbour (kNN) classification approach. The classifier has been trained on a set of partially cloudy images acquired through a melting season. Images, where the calibrations areas are masked out by clouds, will be discharged.

Several papers have demonstrated the potential of SAR for wet snow detection using ERS and Radarsat standard mode (see, e.g., [3] and [4]). Wet snow was detected by utilising the high absorption and therefore low backscatter of wet snow pixels and then comparing the backscatter with the corresponding pixel of a reference scene taken during dry-snow or snow-free conditions. Recently, dry snow has also been inferred by using digital elevation models (DEM) and the wet snow line to postulate dry snow pixels above the wet snow [5]. The methodology has been further improved by taking into account in-situ air temperature measurements and deriving interpolated temperature fields based on standard 6°C per km height-laps rate [6]. A threshold of -3dB has been used with ENVISAT ASAR Wide Swath imagery to detect wet snow.

## 2.2 Baseline multisensor algorithm

The basic idea behind the algorithm is to apply daily optical data and supply with SAR data as frequently as practically possible. SAR data have to be limited to the melting season due to the wet snow requirement. Furthermore, current cost regimes for optical and SAR data will in practice limit the use of SAR data. From practical experience so far, approximately 1-2 SAR image acquisitions per week seem feasible.

The overall algorithm can be written as follows:

$$MSCA_i(x,y) = USCA_i(x,y) \quad (1)$$

for  $i$  which gives  $\max(\text{conf}_{MSCA}(USCA_i(x,y))) \quad i = t, \dots, t-n$

where  $MSCA$  is the new multi-sensor/time-series SCA product,  $USCA$  is a "time-unit" product (a single-sensor product or a day product),  $\text{conf}_{MSCA}$  is a confidence function for multi-sensor/time-series,  $t$  is the current day and  $n$  is the number of days in the time series. In other words, for each pixel  $(x,y)$  select the "best" time unit  $i$  from a time series of unit products. "Best" means the pixel with maximum confidence. Hence, the selection process is entirely controlled by the confidence function. The confidence function,  $\text{conf}_{MSCA}$ , is a decay function of time, i.e., a function giving reduced confidence as the age increases of each unit product. The function might be linear giving largest confidence to today's observations and no confidence above a given time horizon. The two main versions of the multi-sensor/time-series algorithm developed so far and described in the following differ mainly in their way of generating the time-unit products.

## 2.3 NR version

The NR version of the algorithm uses day products for the time-unit products. A day product is defined as a merge of single-image products as follows (pixel indexing has been skipped for clarity):

```
for (each product  $SSCA_i$  of this day) (2)
  if ( $\text{conf}_{DSCA}(SSCA_i) > \text{conf}_{DSCA}(DSCA)$ )
    then  $DSCA = SSCA_i$ 
  else if ( $SSCA_i = \text{CLOUD}$  and  $DSCA = \text{UNCLASS}$ )
    then  $DSCA = \text{CLOUD}$ 
```

Here,  $SSCA$  is a single-image product and  $DSCA$  is the day product (initialized with "UNCLASS"). In other words, if there is one or more cloud-free optical or radar observations for a given pixel position that day, select the single-image product pixel with highest confidence. Otherwise, the pixel is set to "CLOUD". The approach assumes that there in general are multiple acquisitions each day, either optical or a mixture of optical and SAR. It is also assumed that the SCA in practice will not change during the day, which means that multiple observations during a day represent observations of the same snow-cover situation.

The day-confidence function,  $\text{conf}_{DSCA}$ , is the product of the single-image confidence function (for either optical or SAR) multiplied by an inter-product confidence factor. This factor makes it possible to give one sensor different confidence scaling than the other. The image-confidence function is for optical data typically related to the actual spatial resolution of a given pixel (determined by the distance from nadir for a line-scanning instrument), the likelihood of clouds in a pixel (transparent clouds makes mixed pixels) and the assumed snow albedo (which might be quite low late in the melting season).

## 2.4 NORUT version

NORUT has developed a multi-sensor/time-series algorithm which is adapted to near-real-time operation. A new SCA product from the SAR- or optical-processing line will result in an updated multi-sensor product. The current SCA product and its associated confidence map are used as the basis. The new single-image SCA product is subsequently used to upgrade the current multi-sensor/time-series product. The processing line is also able to handle the case when data from different sources arrives at the processing line asynchronously.

## 3 SNOW WETNESS ALGORITHM

The preliminary results from the work on snow surface wetness are currently limited to time-series analysis of optical data, not multi-sensor. The next step will be to integrate the two approaches. The time-series approach applied is presented in the following.

### 3.1 Optical approach

The ideal approach based on optical data would have been to apply a retrieval algorithm for liquid water contents in the snow, like what has been proposed in [7]. However, this would require an imaging spectrometer with optimally located spectral channels for measuring a liquid-water molecular absorption feature. The approach we have used here is to infer wet snow from a combination of measurements of snow temperature (STS) and snow grain size (SGS) in a time series of observations. The temperature observations give a good indication of where wet snow potentially may be present, but are in themselves not accurate enough to provide very strong evidence of wet snow. However, a strong indication of a wet snow surface is a rapid increase of the effective grain size observed simultaneously with a snow surface temperature of approximately 0°C. A simplified version of the algorithm used (more temperature classes are used in practice) is expressed below (pixel indexing has been skipped for clarity):

```

if ( $SGS_{today} - SGS_{recently} > SGS_{snowmelt-tresh}$ )      (3)
  and ( $STS_{low} < STS_{today} < STS_{high}$ ) then
   $MSSW = WET-SNOW$ 
else
  if  $SGS_{today} < SGS_{bare-ground-tresh}$  then
   $MSSW = SNOW-FREE$ 
else
  if  $STS_{today} > STS_{high}$  then
   $MSSW = SNOW-FREE$ 
else
   $MSSW = DRY-SNOW$ 

```

The algorithm also illustrates how bare ground is inferred from temperature observations above 0°C and a rapid developing negative gradient for SGS (both due to appearance of snow-free ground patches at the sub-pixel level). Anyway, we have also applied the SCA product to mask out snow-free areas.

The STS algorithm is based on Key's algorithm ([8] and [9]), which we in a pilot study [10] identified as one of the best single-view techniques for retrieval of STS for polar atmospheres, and it can be applied with MODIS as well as AVHRR and AATSR data. For SGS we used a normalised grain size index based on work in [11] and followed by experiments in [12]. MODIS channels 2 and 7 have been used because the index then has been shown to be less sensitive to snow impurities.

Before calculating SSW, we have to decide the values of a number of parameters. These are threshold values to separate the STS into different classes, a minimum value of SGS to indicate snow-free ground ( $SGS_{bare-ground-tresh}$ ), and an assumed mean increase of SGS per day to indicate a probable melting ( $SGS_{snowmelt-tresh}$ ). All these parameters have to be set experimentally, so those we have applied in our experiments described below are subject for changes.

### 3.2 SAR approach

SAR is very sensitive to snow wetness. By using the same technique as the SCA algorithm for wet snow we achieve a binary wet snow map. This is a first order product, which we initially will use for SAR in our multi-sensor approach. Further development will include a quantitative wet snow product, which indicates the percentage of liquid water in the snow. For single-polarisation SAR imagery this can only be achieved by using a model-based inversion algorithm. The backscattering from snow is a complicated function of surface parameters (roughness, correlation length and wetness), snow parameters (density, depth, grain size and water content) and soil parameters (surface roughness and moisture) in addition to sensor parameters (frequency, polarisation and incidence angle). If the snow is wet, the dominating contribution comes from the snow surface, due to absorption. In [12] algorithms were demonstrated for retrieval of snow wetness from multi-polarisation SAR. For single polarisation SAR (such as ENVISAT ASAR Wide Swath) there are too many parameters involved in the equation to facilitate a full inversion of the problem. Several authors have, however, shown that wet snow can be detected (see [3]).

## 4 EXPERIMENTAL RESULTS

### 4.1 Snow cover area

#### 4.1.1 NR version

The NR version of the SCA multi-sensor/time-series algorithm was first tested for the time period of 9-31 May 2004 when the snowmelt was ongoing in South Norway. For each day there was at least one MODIS image. An optical day product was produced for each day, except for those days when all scenes had to be discharged due to calibration areas masked out by cloud cover (11-14, 17 May). The time series also included 5 ASAR images, from 9, 12, 19, 25 and 31 May 2004.

The optical products yields the SCA as a fraction for each 250 m pixel, while the radar products yields the snow cover as a classification into snow/no-snow for each 100 m pixel. The snow fraction for each 250 m is for the final radar product then derived from the binary classification by resampling. Two types radar products were available for the experiments, one where only observed wet snow were classified as snow, and one where also inferred dry snow were included in the snow class.

The time series analysis were tested and evaluated with confidence values ranging between 0.0 and 1.0 and with a decay factor of 0.1 per day. This means that a pixel with confidence of 0.6 could last for a maximum of 6 days, depending on its initial value. We experimented with different settings of the inter-product confidence for SAR and applied various versions of the product: 1) with

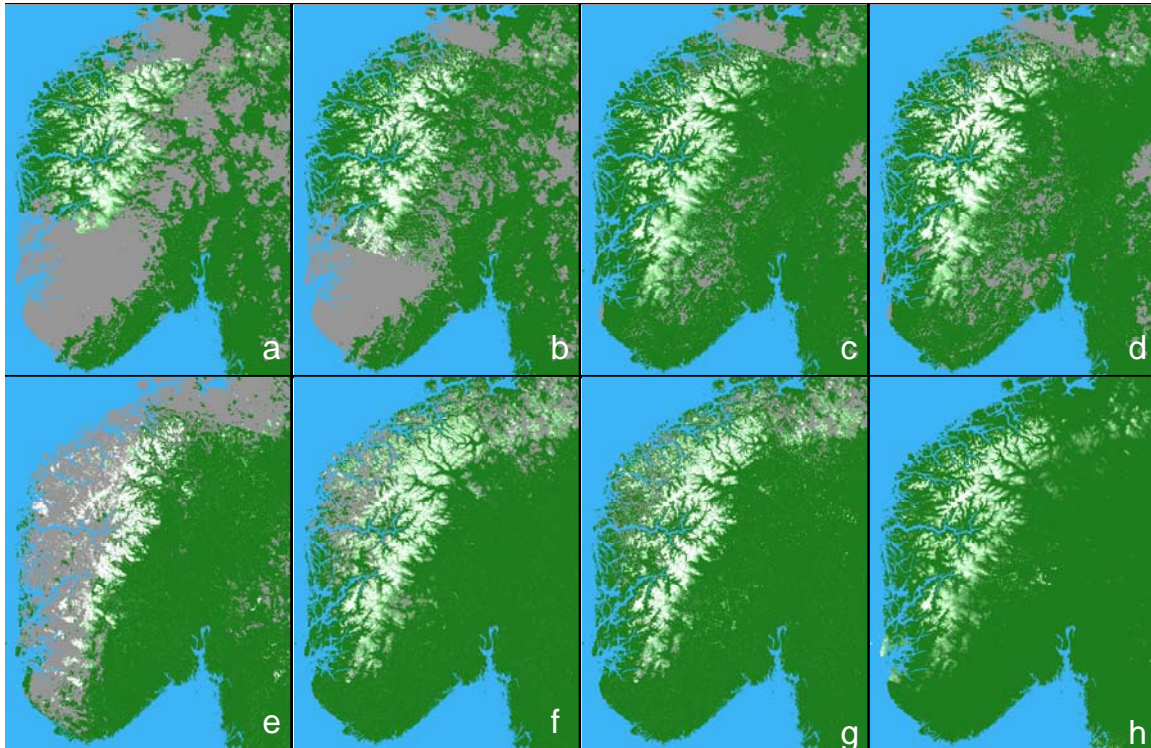


Fig. 1. Multi-sensor/time-series SCA products produced by the NR algorithm. Fractional snow cover is shown on a scale from green (snow free), via tones of green to white (100% snow cover). Clouds and other areas of zero confidence are shown in grey. When not specified, MODIS and ASAR have been used as the data sources. From upper left: a) Optical SCA day product for 9 May 2004; b) Multi-sensor/time-series SCA day product for 9 May 2004. The product consists of optical observations as well as SAR observations; c) 10 May; d) 12 May; e) 19 May. Most of the mountain areas are mapped from the SAR data. Optical data with cloud mask errors cause false snow in the west and south; f) 25 May, with inclusion of optical data only; g) 25 May, also with inclusion of SAR data; h) 31 May, single-image product where MERIS has here been used as the data source (without cloud masking).

dry and wet snow included; 2) with only wet snow included; and 3) entirely without SAR.

In the following, results are presented from the test run where the SAR inter-product confidence was set to 75%, and only wet snow observations were taken into account (see discussion below for these choices).

The first day in the time series is 9 May and consists of an optical day product and as well as a SAR product. Being the first day in a time series, the day product corresponds to a situation where there have been no useful observations for a while. This situation might appear if there are several days of full cloud cover and with only dry snow present in the SAR products. Figure 1a shows the optical day product and Figure 1b the multi-sensor day product. We see that the mapped area was increased by including radar data, and that the two results appear to agree quite well.

When new day products are added to the time-series algorithm, the mapped areas will increase, and the estimated values updated according the confidence

functions. In Figure 1c we see the development of the time-series product the first few days after its initiation. The second day in the time series, 10 May, yielded good optical observations, which updated and confirmed the existing data and increased the mapped area to almost the whole mountain area. The next two days were cloudy. Therefore, there was no day product on 11 May and only a SAR day product on 12 May, see Figure 1d. On 12 May it is clear that the confidence decay function has worked on the existing time-series product. In the western of the map we see that the SAR product has been applied. Note the difference to the east, where the radar product had zero confidence and the existing time-series product was decayed below the threshold (the grey cloud colour). The reason for zero radar confidence here may be presence of forests. Also note that some locations near the coast in the west has been wrongly classified as snow in the radar product.

The period 13-22 May continued to be dominated by clouds, and the daily MSCA had to rely on old products and radar observations. Figure 1e shows the MSCA for

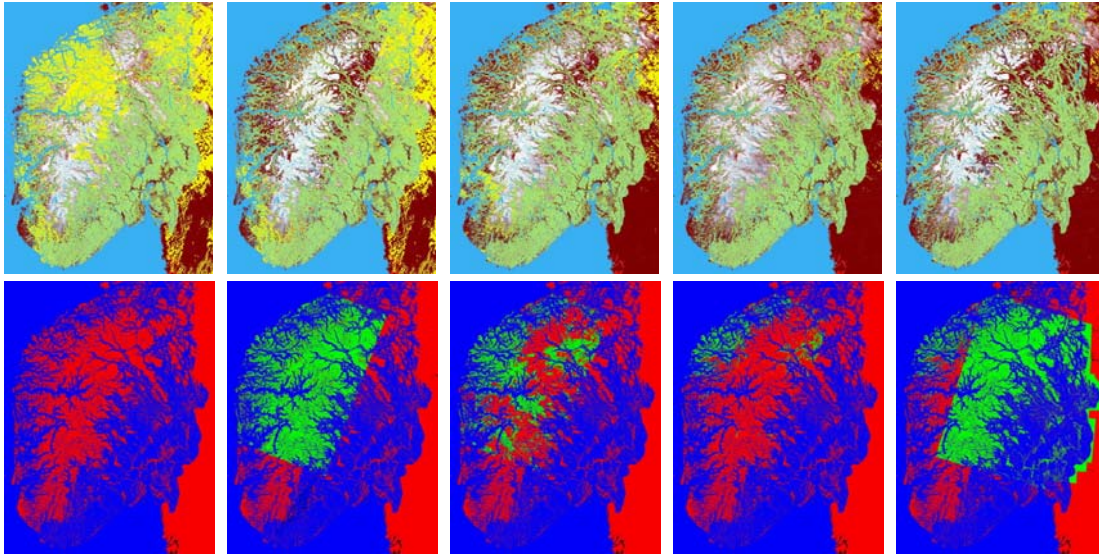


Fig. 2. Product samples from the period 24 April-3 May 2004 produced with the NORUT version of the algorithm (top). Yellow denotes clouds, and is most prominent in the beginning of the period. Green denotes forest mask (non-classified areas). The bottom row shows the source grid for the maps with optical in red, SAR in green and the mask in blue.

19 May, and almost all the snow-covered mountain areas result from optical data. Due to occurrence errors in the cloud mask for optical data, some clouds in the western part are classified as snow covered. The SAR products have identified a lot of snow cover, but these areas are surrounded by unclassified pixels. We cannot say from the product whether those areas actually are snow covered or not.

The optical SCA product for 23 May updated and verified the time-series product in the east and south. An important difference, when utilising optical products compared to radar products, is the ability to estimate fractions of snow cover. The radar SCA gives a more binary result, and yields often a patchy appearance, while the optical data gives a more smooth appearance.

The time-series product of 25 May is shown in two different versions, one with optical data only (Figure 1f), and one where also SAR data have been included (Figure 1g). The SAR data improves the classification in the northwest by identifying snow-covered areas as well as snow-free areas. Note that in the eastern part of the radar product some strange patches of snow within the snow-free areas appear.

In Figure 1h we show the last product in the test. From 27 May the sky was mainly cloud free in large parts of the area. The last day product of 31 May used here is based on MERIS data. Since MERIS does not allow detection of clouds over snow-covered surfaces, it is hard to use this sensor operationally. However, this

product indicates that SCA retrieval from MERIS works as well as for MODIS.

#### 4.1.2 NORUT version

Figure 2 shows an example of multi-sensor/time-series SCA product based on the NORUT version of the algorithm. In addition to the SCA product an image indicating the source is also shown. The multi-sensor/time-series confidence map is also shown. For demonstration near real-time multi-sensor/time-series products were produced for the period 20 April-31 June 2004. Each time a new single-image product was made a multi-sensor/time-series product was also produced. The decay function was set last one week.

In Figure 2 product samples from the period 24 April-3 May are displayed. Areas without SAR coverage is clearly more clouded than areas with SAR coverage. When studying the details of the products it is also evident that pixels with contribution from SAR have a higher contrast (typically either 0% or 100% SCA) than for optical contributions.

## 4.2 Snow surface wetness

### 4.2.1 Optical version

The optical SSW algorithm has been tested on a time series of MODIS images from April 2003. For each day in the period STS and SGS have been calculated from MODIS L1B data with pixel size 1 km. The inference of SSW for a certain date has been done using the STS and

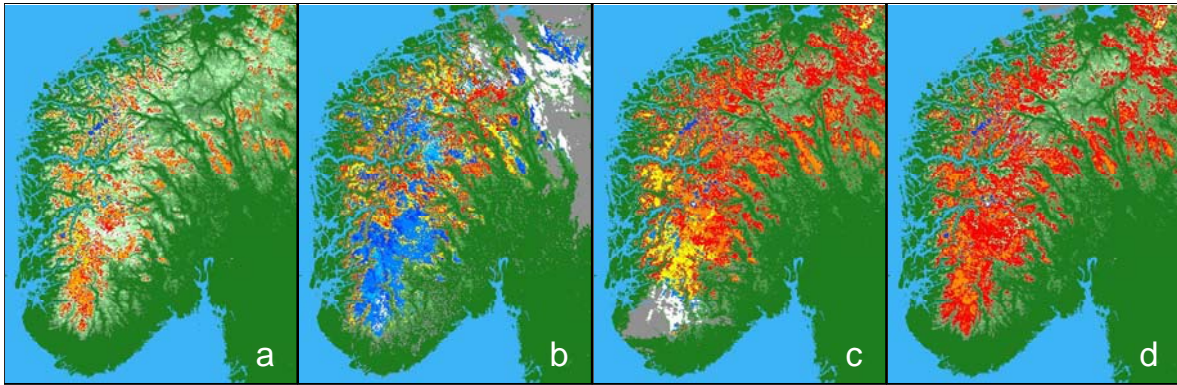


Fig. 3. SSW products for four days in 2003 produced by the NR version of a time-series algorithm. There are four temperature classes: (1) Dry, cold snow (white), (2) dry/moist (blue/light blue), (3) moist (orange/yellow) and (4) wet (red). For classes 2 and 3 blue and orange means constant grain size and light blue and yellow means increasing grain size. The figure shows from left to right: a) 30 April; b) 16 April; c) 20 April; and d) 22 April. The STS threshold was  $+1^{\circ}\text{C}$  for map a and  $+3^{\circ}\text{C}$  for maps b-d.

SGS for the current day and the SGS from one until a few days before.

The classification is done for each pixel using the calculated STS and the size of the variation of the grain size index. Four temperature classes have been used with the following threshold values: dry/cold snow ( $< -2^{\circ}\text{C}$ ), dry/moist snow ( $> -2^{\circ}\text{C}$  and  $< -0.5^{\circ}\text{C}$ ), moist snow ( $> -0.5^{\circ}\text{C}$  and  $< +0.5^{\circ}\text{C}$ ) and wet snow ( $> +0.5^{\circ}\text{C}$  and  $< +1.0^{\circ}\text{C}$ ). Each of these classes has subclasses according to the variation of the SGS: decreasing SGS, constant SGS, increasing SGS (more than an assumed mean value per day) and unknown (no value to compare with). In addition the classification gives indications of snow-free ground present.

The classification is done for each pixel. A class value cannot be calculated if today's pixel is covered with clouds. After calculation STS and SGS values, the possibility of snow-free ground is checked. Then the SGS value is compared with the SGS from yesterday. If yesterday's pixel is covered with clouds, the SGS difference is unknown. Then the algorithm goes back to the day before and successively backwards up to the maximum number of days set (we have used a maximum of 5 days).

In Figure 3a the classification result is added on top of the SCA maps. 100% SCA is shown in white, and the decreasing percentage of snow cover is shown in green with increasing darkness. Note that there are large snow covered areas that have not been classified. In particular, one can observe areas with 100% snow cover which are unclassified due to the sensitivity effect of STS and SGS to fractional snow-free ground, as mentioned above.

If we increase the STS upper threshold to  $+3^{\circ}\text{C}$ , the areas with assigned class values will increase substantially. In Figure 3b-d this threshold has been

used. The figures show the development through the period from 16-22 April 2003 in South Norway. Before this week there had been a long period of cold weather, but during these days the temperature increased and the snowmelt started.

In Figure 3b one can see that in the south and in the highest mountain areas the snow is starting to get warmer and is not far from  $0^{\circ}\text{C}$  (blue). There are only a few small areas with cold dry snow (white). In the north-eastern part one can see larger white areas, but this may be due to erroneous cloud detection. The temperature of the clouds is far below zero. In other areas the melting has probably started. There are large orange/yellow areas and some red.

Four days later, the melting is going on in the entire region (Figure 3c). Errors in the cloud detection can be seen in the south. The white area is certainly clouds and not dry snow.

Figure 3d shows that there probably was wet snow almost everywhere. Only on the highest glacier areas we can see some blue and white pixels. If we compare with Figure 3a, we can see the result of using the  $+3^{\circ}\text{C}$  threshold instead of  $+1^{\circ}\text{C}$  as upper temperature limit.

#### 4.2.2 SAR version

The SAR SSW algorithm has been run continuously in parallel with the SAR SCA algorithm, and has produced 16 SSW products through the snowmelt season. The time series has been studied and shows consistent time behaviour. Comparisons with in-situ measurements from the 2004 field season are planned.

Figure 4 shows a comparison between the SAR wet-snow product from 25 May 2004 and the MODIS wet snow product from 26 May 2004. The same features are

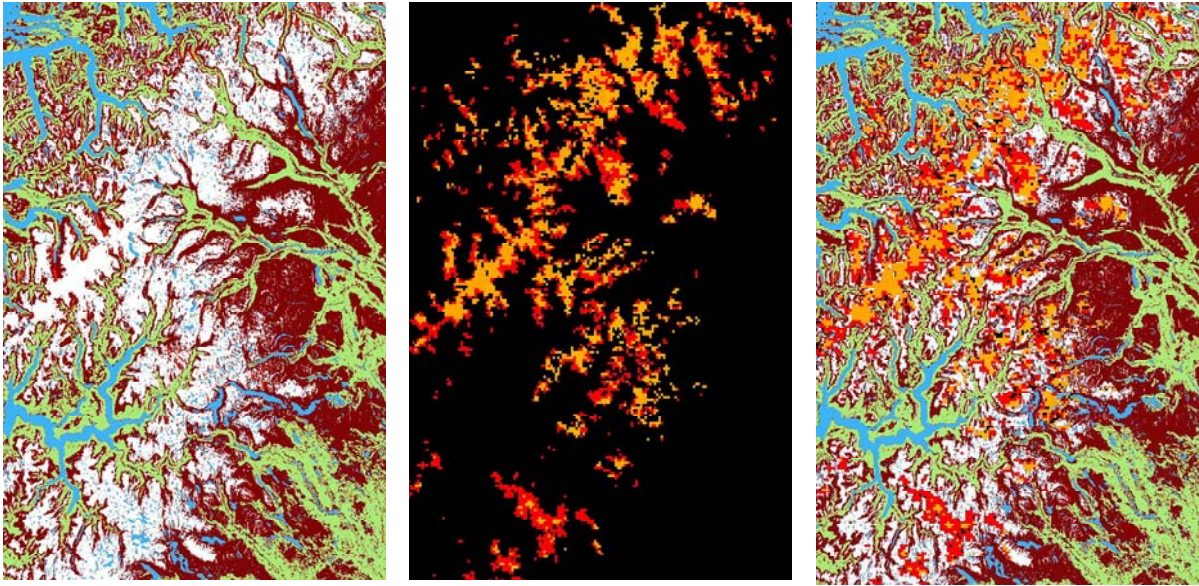


Fig. 4. Comparison between SAR wet-snow product from 25 May 2004 (left) and the MODIS wet snow product from 26 May 2004 (middle). The map on the right shows the wet snow retrieved from optical data superimposed onto the SAR-based map for comparison. It is clear that the optical algorithm predicts less wet snow than the SAR algorithm.

recognisable in each image, but there are also large differences. The SAR wet snow algorithm detects in general more wet snow than the optical algorithm.

## 5 DISCUSSION AND CONCLUSIONS

### 5.1 Snow cover area

The first experience with the NR version of the multi-sensor/time-series algorithm shows that the results depend very much on how the initial single-image product confidence is set and on the time decay function. It appears that closeness to clouds should have been given reduced confidence in the optical data in order to reduce the risk of classifying clouds as snow. More important, however, is to consider how to fuse the SAR and optical products better.

When optical data are unavailable due to clouds, the use of radar data improves the product by covering larger areas. Due to the binary character of the radar products, some omission of snow (probably due to high-backscattering objects in some SAR pixels) and the limitation to only detect wet snow, we have set the inter-product confidence value for SAR to a lower value than for optical. We examined and evaluated various inter-product confidence factors for SAR, and we found that factors below 0.5 clearly reduced the contribution from the SAR products too much. Using a value close to 1.0 preserved too much of the binary pattern from the ASAR products. This means that high confidences for SAR had a tendency to override subsequent optical products. We

found that a factor of 0.75 was a good compromise between preserving results from the optical sensors and including results from radar products when needed.

We examined the effect of including assumptions about dry snow in the radar product. Using a SAR SCA product including also inferred dry snow appeared to overestimate the snow cover compared to the optical product. Using SAR SCA based on wet snow only appeared to slightly underestimate the snow cover compared to the optical product. We also tried to reduce the confidence of SAR pixels classified as dry snow, but this did not improve the result significantly.

Some experiments were performed with MERIS data instead of MODIS. The MERIS-based single-scene SCA maps seem to be of similar quality as the MODIS-based maps for cloud-free conditions. However, clouds make serious problems over snow covered surfaces since MERIS does not have the spectral bands needed to separate snow and clouds spectrally. AATSR can be used for generating a cloud mask, but it would, unfortunately, only cover a part of the MERIS image. If one limits the use of the MERIS image to the area covered by AATSR, less frequent coverage would be a consequence.

The experience with the NORUT version of the SCA algorithm confirms that interpretation of SCA from SAR imagery is not as straightforward as for optical imagery. In the original 100 m SAR product the wet snow threshold is binary (wet snow/non-wet snow). Due to the logarithmic coding of backscatter in SAR imagery a small fraction of bare ground in a SAR pixel may cancel

out a large fraction of snow. Also, the resampling of 100 m products to 250 m generates fractional snow coverage where bare ground, wet and dry snow and maybe also mask pixels are combined into a snow-cover fraction. There is a need to harmonise the fusion of SAR and optical SCA retrieval better in the future.

In spite of the abovementioned problems, the results of the study showed that SAR-based maps in general were fairly consistent with optical-based maps. The SAR-based maps were very useful for updating the multi-sensor/time-series products in a period of missing optical observations. The SAR observations were to a large degree confirmed by subsequent optical SCA observations. However, for some places the SAR wet SCA values had a tendency to underestimate the SCA, compared to optical data. When dry snow estimates were included in the radar products, the tendency was the opposite.

## 5.2 Snow surface wetness

The optical experiments done so far have confirmed that the approach of combining STS and SGS, analysed in a time series of observations, can be used to infer wet snow, including giving an early warning of snowmelt start. Air temperature measurements from meteorological stations confirm the maps produced in general. The main problems observed so far are related to clouds. In some maps it is observed that dry and cold snow is more frequent close to clouds. One could imagine that this is because the clouds have kept the sunlight away – hence the snow has not been warmed. But it might as well be that parts of the clouds have not been detected. The problems are typically associated with transparent clouds.

The calculated SGS index does not give the precise size of the snow grains, but is an indication of the grain size. The value of the SGS index increases with increasing grain size. For a pixel totally covered with snow, the SGS index is a good indication of the grain size. Bare ground gives a low value for the SGS index. This means that for a pixel only partly covered with snow, we could measure a low SGS index even for large snow grain sizes. A decreasing value of SGS could mean new fallen snow or increasing snow-free area.

For STS there is a similar problem. With a snow temperature of 0°C, the snow will start to melt and the temperature will stop increasing. For a pixel only partly covered with snow, the temperature of the snow-free area will influence, resulting in measured STS values some degrees above 0°C. This will usually mean that the snow is wet, but if the snow-free area is sufficiently large, one can measure an average positive temperature for the pixel even if the snow is cold and dry.

Therefore, a good estimate of SSW is valid only for pixels completely covered with snow. An accurate SCA map should be used to restrict the pixels classified. We

assume that the SSW estimate is reasonable good even if there are small areas of bare ground included.

The SAR experiments have confirmed that SAR can be used to detect the presence of wet snow. The generation of quantitative correct products is in development. For very accurate estimates, there is a need to invert a simplified backscatter models to obtain approximate correct results for the liquid water content in the snow surface.

A first comparison between SSW products derived from SAR and optical sensors has been carried out. There are large differences between the two products. The optical based algorithm seems to predict less wet snow than the SAR algorithm. It is too early to conclude why this is so, but we expect to harmonise the results when the reason for the difference is better understood.

## 6 ACKNOWLEDGMENT

The authors like to thank the colleagues in NR and NORUT that contributed to the fieldwork in several campaigns in 2003 and 2004. The work behind this paper has partly been funded by the European Commission projects EnviSnow and EuroClim and the Norwegian Research Council project SnowMan. The ENVISAT data were funded by the ESA ENVISAT AO no. 785.

## 7 REFERENCES

1. T. Andersen, Operational snow mapping by satellites, Hydrological aspects of alpine and high mountain areas, *Proceedings of the Exeter symposium*, July 1982, IAHS publ. no. 138, pp. 149-154.
2. R. Solberg and T. Andersen, An automatic system for operational snow-cover monitoring in the Norwegian mountain regions, *Geoscience and Remote Sensing Symposium (IGARSS)*, Pasadena, California, USA, 1994.
3. T. Nagler and H. Rott, Retrieval of wet snow by means of multitemporal SAR data, *IEEE Transactions of Geoscience and Remote Sensing*, Vol. 38, No. 2, March 2000, pp. 754-765.
4. J. Koskinen, S. Metsämäki, J. Grandell, S. Jänne, L. Matikainen and M. Hallikainen, Snow monitoring using radar and optical satellite data, *Remote Sensing of Environment*, vol. 69, no. 1, pp. 16-29, 1999.
5. E. Malnes and T. Guneriusen, Mapping of snow covered area with Radarsat in Norway, *Geoscience and Remote Sensing Symposium (IGARSS)*, 24-28 June 2002, Vol. 1.
6. E. Malnes, R. Storvold and I. Lauknes, Near real time snow covered area mapping with Envisat ASAR widenswath in Norwegian mountainous areas, *ESA*

*ENVISAT & ERS Symposium*, Salzburg, Austria, September 6-10, 2004.

7. R.O. Green and J. Dozier, Measurement of the spectral absorption of liquid water in melting snow with an imaging spectrometer, *Summaries of the Fifth Annual JPL Airborne Earth Science Workshop*, January 23-26, 1995, JPL Publication no. 95-1, pp. 91-94.

8. J. R. Key, J. B. Collins, C. Fowler, and R. S. Stone, High-latitude surface temperature estimates from thermal satellite data, *Remote Sensing of Environment*, 1997. 61(2), pp. 302-309.

9. J.R. Key, Polar surface temperature retrieval from space: coefficients, <http://stratus.ssec.wisc.edu/products/surftemp/surftemp.html>, 2003.

10. J. Amlien and R. Solberg, A comparison of temperature retrieval algorithms for snow covered surfaces, *Geoscience and Remote Sensing Symposium (IGARSS)*, Toulouse, France, 21-25 July 2003.

11. J. Dozier, Spectral signature of alpine snow cover from the Landsat Thematic Mapper, *Remote Sensing of Environment*, vol. 28, pp. 9-22, 1989.

12. M. Fily, B. Bourdelles, J.P. Dedieu, C. Sergent, Comparison of In Situ and Landsat Thematic Mapper Derived Snow Grain Characteristics in the Alps, *Remote Sensing of Environment*, Vol. 59, No. 3, p. 452-460.

13. J. Shi and J. Dozier, Inferring snow wetness using C-band data from SIR-C polarimetric SAR, *IEEE Transactions of Geoscience and Remote Sensing*, vol. 33, pp. 905-914, 1995.